

30 **Abstract**

31 Voltage-gated sodium ion channels allow for the initiation and transmission of action potentials.
32 There is a high interest in research and drug development to selectively target these ion
33 channels to treat epilepsy and other disorders such as pain. Scientific literature and
34 presentations often incorporate maps of these integral membrane proteins with markers
35 indicating gene mutations to highlight genotype/phenotype correlations. There is a need for
36 automated tools to create high quality figures with mutation (variant) locations displayed on
37 these channel maps. This manuscript introduces a simple application to create visualization for
38 mutations on alpha voltage-gated sodium channels, created using the D3.js library. The
39 application allows for mapping of variant sequences, as well as important properties like the
40 type of variant and the phenotypes linked to the variant. It also allows for customizability and
41 the production of high-quality images for publication. This application and code base can
42 further be extrapolated to other ion channels as well.

43

44

45

46

47

48

49

50

51

52

53

54

55

56

57

58

59

60

61 **Introduction**

62 *Role of Voltage-Gated Sodium Ion Channels in Physiology*

63 Voltage-gated sodium ion channels are integral membrane proteins that induce the rising phase
64 of the action potential in most electrically excitable cells, including neurons (Catterall, 2000).
65 The channel first opens, allowing sodium ions to flow into the cell and depolarizing the cell
66 membrane potential. Opening is followed by a conformational change to inactivated states,
67 preventing further sodium influx and allowing repolarization (Armstrong, 2006; Oliva et al.,
68 2012). As a result, gain- or loss-of-function mutations in these ion channels result in abnormal
69 excitable cell activity and leads to varied disorders in the nervous system, skeletal muscle, and
70 cardiac tissue (Fouda et al., 2022; Meisler et al., 2021; Stafstrom, 2007).

71 *Structure of Sodium Channels*

72 Graphical representations of sodium channels are often incorporated into scientific literature,
73 where they are depicted as having four domains (DI – DIV) with six transmembrane segments
74 (S1-S6) in each (Catterall & Swanson, 2015). Segments S1-S4 compose the voltage sensor region
75 with S4 being the positively charged segment that dynamically shifts in response to
76 depolarization inducing the opening (or inactivation) of the channel and the initiation of (or
77 cessation of) sodium influx (Peters et al., 2016). Segments S5 and S6, with the intervening re-
78 entrant P loop, create the pore forming region (Peters et al., 2016; Sands et al., 2005).

79 *Related Work*

80 Despite the common occurrence of figures for sodium channels in publications, there are few
81 applications that generate diagrams of these proteins automatically. Many of these diagrams
82 are annotated by hand (Goldberg et al., 2007) or manually created through an image editing or
83 presentation program such as PowerPoint (Catterall, 2012; Meisler & Kearney, 2005; Oliva et al.,
84 2012). The few applications that exist specifically for producing figures of voltage-gated
85 channels require the user to place mutation sequences in position manually or require the data
86 to be in a specific format that is inaccessible and unintuitive to most users. TopDraw (Bond,
87 2003), for example, allows for easy sketching of protein topologies, but it does not provide the
88 ability to annotate and is solely used to derive a sketch from another source such as HERA.
89 TOPO2 (Johns, 2010) is unable to predict the location of the transmembrane segments and only
90 exports the figure as a PNG, which is a raster image format that is sometimes not accepted by
91 publishers. Similarly, NaView (Afonso et al., 2022) generates a visualization automatically and
92 provides customizability by allowing the user to alter colors and text position, but annotations
93 need to be manually added. Furthermore, user-provided input must be a UniProt formatted
94 string and/or a JSON object, which may be inaccessible or tedious for most users.

95 In comparison, this Variant Mapping application is a user-friendly D3.js and React.js application
96 that can be used to automatically generate a scaled SVG figure of a sodium channel with
97 annotations for mutation sequences, custom labels, and legends. The application also allows

98 custom color selection, filters, toggles, and sliders that can be used to customize the image
99 before exporting to a PNG or SVG file at resolutions acceptable for journal submission.

100

101 **Methods and Results**

102 *Link to Application:* [Variant Mapping Application\(ionchannel-biology.github.io\)](https://ionchannel-biology.github.io)

103 *Technologies Used*

104 The Variant Mapping application primarily uses a combination of D3.js and React.js, which are
105 both JavaScript libraries. D3.js, also known as D3 or Data-Driven Documents, uses web
106 standards like HTML, CSS, and SVG to produce dynamic, interactive, and customized data
107 visualizations. The library is particularly powerful in data manipulation and is extremely fast due
108 to its minimal overhead in that it only modifies the attributes that change. This makes it an ideal
109 choice for mathematical functions, analytical tasks, animations, data manipulation, and scaling
110 of data within applications to create beautiful and powerful visualizations. React.js, also known
111 as React, is the other library used and is often utilized to create interactive websites and build
112 user interfaces through the production of components. Since the D3 community has not yet
113 established a standard way to create components, React is ideal to control the rendering and re-
114 rendering of elements.

115 While integrating D3 and React can be tricky because they both want to manipulate the DOM
116 (Battle et al., 2021), doing so makes the code declarative instead of imperative (Wattenberger,
117 2022). The integration also allows for most components to be separated, making the elements
118 reusable and the application is more scalable for future updates.

119 *Structure and Features*

120 Data on the structure of sodium channels is sourced from UniProt and converted to a *.csv file.
121 The file contains information on the size of the membrane and paths, as well as the relative
122 locations for markers when mutation sequences are later input. The relationship between the
123 elements in the D3 layout is the same as the relationship between the domains, segments, and
124 loops depicted in current literature. The domains are each a group element, the
125 transmembrane segments are rectangles within each domain group, and the loops are path
126 elements in their respective domains. The loops are also scaled proportional to the extracellular
127 and cytoplasmic regions of the protein. D3 provides an advantage here because the path tag
128 allows for the ability to create scalable curves, whereas plain HTML does not have equivalent
129 functionality (Sweeny, 2018).

130 There are two main inputs for the user to supply their own data: a form for inputting mutational
131 sequences one at a time (Figure 1) and an input to upload an Excel or CSV file. The option to
132 upload Excel files is more accessible compared to earlier applications, where users only had the

133 option to import UniProt code or JSON objects, since most users will have access to Microsoft
134 Excel. This option also provides a quicker alternative to users to upload data if they wish.

135 A [colour picker](#), is added for additional customizability and for users to have the flexibility to
136 decide the story they want to tell with their data. For example, users can select darker colours
137 for more severe diagnoses and lighter colours for less severe diagnoses. In another instance,
138 users may select warm colours for loss of function mutations and cool colours for gain of
139 function mutations.

140 Additionally, the legend has added filters where the user can select the text for the specific
141 mutations they want. This is for added customizability and to provide users with an easier
142 solution to spot patterns between similar types of mutations or diagnoses. Moveable text
143 labels, toggles, and a slider for the legend position have also been added for customizability.

144 The Variant Mapping application will be hosted on a public server and can be accessed locally
145 on any computer [Variant Mapping Application \(ionchannel-biology.github.io\)](#). The application
146 produces a figure of the desired sodium channel and a table containing the user-input data
147 along with the addition of a domain label and region label (Figure 1). Users can also choose to
148 download the figure as a PNG or SVG (Figure 2) and export the table as an Excel spreadsheet
149 (Figure 3).

150 **Discussion**

151 In this current work, we demonstrate the Variant Mapping application and are providing public
152 access to the application. We believe this work sets a foundation for generation of other similar
153 tools that not only ease production of high-quality figures but can also be used as a learning
154 tool for understanding ion channel mutations. Future updates could focus on extrapolating to
155 other voltage-gated ion channel families such as calcium and potassium channels. The current
156 code could also be altered to become more flexible by adding the beta subunits of the sodium
157 channels. In summary, we are excited to provide this tool as an open access application to the
158 scientific community and we hope this encourages other similar work that will aid in the
159 advancements in precision medicine and provide a valuable learning tool for students of ion
160 channel function and dysfunction.

161

Enter Mutation Data

Sequence
D1714V

Mutation Type
Missense

Phenotype
LO-DS

Marker Size

Submit

Mutation Table

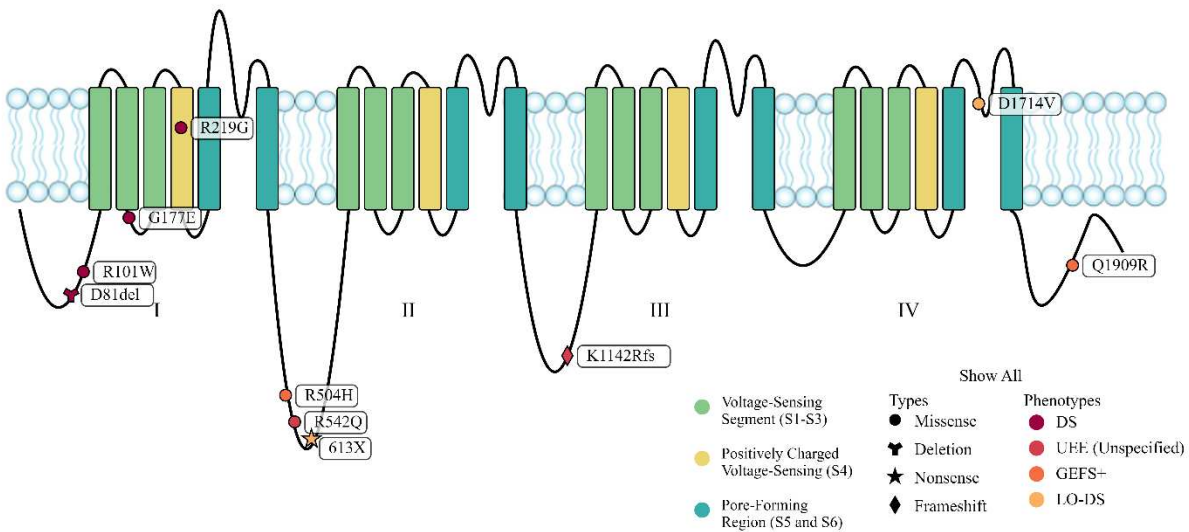
Delete from table

Select	Sequence	Type	Phenotype	Domain	Region
<input type="checkbox"/>	R101W	Missense	DS	N/A	Cytoplasmic
<input type="checkbox"/>	G177E	Missense	DS	I	Cytoplasmic
<input type="checkbox"/>	R219G	Missense	DS	I	S4
<input type="checkbox"/>	D81del	Deletion	DS	N/A	Cytoplasmic
<input type="checkbox"/>	R542Q	Missense	UEE (Unspecified)	N/A	Cytoplasmic
<input type="checkbox"/>	R504H	Missense	GEFS+	N/A	Cytoplasmic
<input type="checkbox"/>	613X	Nonsense	LO-DS	N/A	Cytoplasmic
<input type="checkbox"/>	Q1909R	Missense	GEFS+	N/A	Cytoplasmic
<input type="checkbox"/>	K1142Rfs	Frameshift	UEE (Unspecified)	N/A	Cytoplasmic
<input type="checkbox"/>	D1714V	Missense	LO-DS	IV	Pore-forming

162

163 *Figure 1: Form and Resulting Table*

164 Users enter mutation data in the form on the left. The table on the right shows an example of what is displayed after entering
 165 multiple mutation sequences.



166

167 *Figure 2: Resulting Figure with Multiple Markers*

168 The figure that is produced when the user exports the diagram as a PNG or SVG. Before exporting, users can customize the
 169 figure by moving the labels, altering the colors, filtering the visible mutations, and toggling the legend on/off.

A	B	C	D	E	F
Select	Sequence	Type	Phenotype	Domain	Region
	R101W	Missense	DS	N/A	Cytoplasmic
	G177E	Missense	DS	I	Cytoplasmic
	R219G	Missense	DS	I	S4
	D81del	Deletion	DS	N/A	Cytoplasmic
	R542Q	Missense	UEE (Unspecified)	N/A	Cytoplasmic
	R504H	Missense	GEFS+	N/A	Cytoplasmic
	613X	Nonsense	LO-DS	N/A	Cytoplasmic
	Q1909R	Missense	GEFS+	N/A	Cytoplasmic
	K1142Rfs	Frameshift	UEE (Unspecified)	N/A	Cytoplasmic
	D1714V	Missense	LO-DS	IV	Pore-forming

170

171 *Figure 3: Resulting Excel Spreadsheet*

172 The spreadsheet of the user-inputted mutations after exporting the displayed table to an XLSX file.

173

174 **Data availability statement:** The raw data supporting the conclusions of this article will be made
175 available by the authors, without undue reservation.

176 **Acknowledgments:** We would like to thank the entire Xenon family for their support of this
177 work.

178 **Author contributions statement:** JPJ conceived this work. WW and AM wrote the code and
179 designed the visualizations. RD and AC provided the raw data for the application and RD, AC,
180 and RRP advised on the project. WW, AM, and RRP wrote the manuscript. All authors edited and
181 approved the final draft.

182 **Funding:** This project was funded by Xenon Pharmaceuticals Inc.

183 **Conflict of interest statement:** All authors are employees of Xenon Pharmaceuticals Inc. and
184 may hold stock or stock options in the Company.

185

186 **References**

- 187 Afonso, M. Q. L., da Fonseca Júnior, N. J., Miranda, T. G., & Bleicher, L. (2022). Naview: A d3.js
188 Based JavaScript Library for Drawing and Annotating Voltage-Gated Sodium Channels
189 Membrane Diagrams. *Frontiers in Bioinformatics*, 2. <https://doi.org/10.3389/fbinf.2022.774417>
- 190 Armstrong, C. M. (2006). Na channel inactivation from open and closed states. *Proceedings of*
191 *the National Academy of Sciences*, 103(47), 17991–17996.
192 <https://doi.org/10.1073/pnas.0607603103>
- 193 Battle, L., Feng, D., & Webber, K. (2021). Exploring Visualization Implementation Challenges
194 Faced by D3 Users Online, 1–21. <https://doi.org/10.48550/arXiv.2108.02299>
- 195 Bond C. S. (2003). TopDraw: a sketchpad for protein structure topology cartoons. *Bioinformatics*
196 (Oxford, England), 19(2), 311–312. <https://doi.org/10.1093/bioinformatics/19.2.311>
- 197 Catterall W. A. (2000). From ionic currents to molecular mechanisms: the structure and function
198 of voltage-gated sodium channels. *Neuron*, 26(1), 13–25. [https://doi.org/10.1016/s0896-](https://doi.org/10.1016/s0896-6273(00)81133-2)
199 [6273\(00\)81133-2](https://doi.org/10.1016/s0896-6273(00)81133-2)
- 200 Catterall, W.A. (2012), Voltage-gated sodium channels at 60: structure, function and
201 pathophysiology. *The Journal of Physiology*, 590: 2577-
202 2589. <https://doi.org/10.1113/jphysiol.2011.224204>
- 203 Catterall, W. A., & Swanson, T. M. (2015). Structural Basis for Pharmacology of Voltage-Gated
204 Sodium and Calcium Channels. *Molecular pharmacology*, 88(1), 141–150.
205 <https://doi.org/10.1124/mol.114.097659>
- 206 Fouda, M. A., Ghovanloo, M., & Ruben, P. C. (2022). Late sodium current: incomplete
207 inactivation triggers seizures, myotonias, arrhythmias, and pain syndromes. *The Journal of*
208 *Physiology*, 600(12), 2835–2851. <https://doi.org/10.1113/JP282768>
- 209 Goldberg, Y., MacFarlane, J., MacDonald, M., Thompson, J., Dube, M.-P., Mattice, M., Fraser, R.,
210 Young, C., Hossain, S., Pape, T., Payne, B., Radomski, C., Donaldson, G., Ives, E., Cox, J.,
211 Younghusband, H., Green, R., Duff, A., Boltshauser, E., Grinspan, G., Dimon, J., Sibley, B., Andria,
212 G., Toscano, E., Kerdraon, J., Bowsher, D., Pimstone, S., Samuels, M., Sherrington, R. and
213 Hayden, M. (2007), Loss-of-function mutations in the Nav1.7 gene underlie congenital
214 indifference to pain in multiple human populations. *Clinical Genetics*, 71: 311-
215 319. <https://doi.org/10.1111/j.1399-0004.2007.00790.x>
- 216 Johns, S. J. (2010). TOPO2, Transmembrane Protein Display Software. Available
217 at: <http://www.sacs.ucsf.edu/TOPO2/>.
- 218 Ioannis C. Spyropoulos, Theodore D. Liakopoulos, Pantelis G. Bagos and Stavros J. Hamodrakas
219 TMRPres2D: high quality visual representation of transmembrane protein models
220 *Bioinformatics*. 2004; 20: 3258-3260.

- 221 Meisler, Miriam H. & Kearney, Jennifer A. (2005). *J Clin Invest.* [115\(8\)](#):2010-
222 2017. <https://doi.org/10.1172/JCI25466>.
- 223 Meisler, M. H., Hill, S. F., & Yu, W. (2021). Sodium channelopathies in neurodevelopmental
224 disorders. *Nature Reviews Neuroscience*, 22(3), 152–166. [https://doi.org/10.1038/s41583-020-](https://doi.org/10.1038/s41583-020-00418-4)
225 [00418-4](https://doi.org/10.1038/s41583-020-00418-4).
- 226 Oliva, M., Berkovic, S.F. and Petrou, S. (2012), Sodium channels and the neurobiology of
227 epilepsy. *Epilepsia*, 53: 1849-1859. <https://doi.org/10.1111/j.1528-1167.2012.03631.x>
- 228 Peters, C., Rosch, R., Hughes, E. et al. (2016). Temperature-dependent changes in neuronal
229 dynamics in a patient with an SCN1A mutation and hyperthermia induced seizures. *Sci*
230 *Rep* 6, 31879. <https://doi.org/10.1038/srep31879>.
- 231 Sands, Z., Grottesi, A., & Sansom, M. S. (2005). Voltage-gated ion channels. *Current biology:*
232 *CB*, 15(2), R44–R47. <https://doi.org/10.1016/j.cub.2004.12.050>.
- 233 Stafstrom, C. E. (2007). Persistent Sodium Current and Its Role in Epilepsy. *Epilepsy Currents*,
234 7(1), 15–22. <https://doi.org/10.1111/j.1535-7511.2007.00156.x>
- 235 Sweeney, P. (2018, December 16). Why I no longer use D3.js [web log]. Retrieved June 14, 2022,
236 from <https://medium.com/@PepsRyuu/why-i-no-longer-use-d3-js-b8288f306c9a>
- 237 D3 color picker w/ button: <https://embed.plnkr.co/xP6nHx/>
- 238 Usluer, S., Salar, S., Arslan, M., Yiş, U., Kara, B., Tektürk, P., Baykan, B., Meral, C., Türkdoğan, D.,
239 Bebek, N., Yalçın Çapan, Ö., Gündoğdu Eken, A., & Çağlayan, S. H. (2016). SCN1A gene
240 sequencing in 46 Turkish epilepsy patients disclosed 12 novel mutations. *Seizure*, 39, 34–43.
241 [https://www.seizure-journal.com/article/S1059-1311\(16\)30043-7/fulltext](https://www.seizure-journal.com/article/S1059-1311(16)30043-7/fulltext)
- 242 Wattenberger, A. (2022). React + D3.js. Wattenberger. Retrieved June 16, 2022, from
243 <https://wattenberger.com/blog/react-and-d3>